

# Zfish Paper 1

Ashwin, Kayvon, Alex, Emre and Sebastian

February 26, 2016

## Abstract

For the eyes to remain still between saccades, there exists cells in the hindbrain that fire in a persistent manner for the duration of the gaze. These cells perform the task of integration, in that their inputs are eye velocity signals and their output is eye position signals. How these cells perform this task is the focus of the study. To study this circuit we used two-photon microscopy in combination with serial electron microscopy to map the function of velocity-to-position-integrator (VPNI) neurons in the hindbrain of larval zebrafish onto the ultrastructure of the same neurons. Hindbrain neurons of larval zebrafish were imaged while the animal made spontaneous saccades. The same neurons were then identified and reconstructed at the ultrastructure level. Our reconstructions revealed VPNI cells with varied dendritic morphologies, axonal projections and synaptic distributions, over a large range of persistence time constants. We observed that cells located rostrally had ipsilaterally projecting axons while cells that were caudal had contralaterally projecting axons. We also observe, the first evidence of synapses among integrator neurons, specifically from the ipsilaterally projecting cells onto other ipsilateral cells and from ipsilaterally projecting cells onto contralateral cells. The axons of these cells tend to have 'clustered' presynaptic sites onto dendrites from different cells. The neurotransmitter identity of these VPNI cells can be inferred by somatic locations of cells that are known to follow a stereotypic expression pattern in larval zebrafish. Based on this, we speculate that cells with ipsilaterally projecting axons were largely excitatory, where as cells with contralaterally projecting axons were inhibitory. Together, these observations are beginning to reveal the structure of the circuit that can support neural integration in the larval zebrafish.

## 1 Introduction

The ability to hold ones eye at a certain location in space is a remarkable feat. This is achieved by groups of neurons in the brainstem, that precisely control the motor neurons that innervate the eye-muscles. The inputs to these neurons are saccadic commands that encode for eye position, where as the output of these neurons is tonic firing proportional to the eye position. In other words, the input is a burst like command signal to the neuron and the output is a step like persistent firing from the neuron. In mathematical terms this is the act of integration and these neurons perform the task of temporal integration. This phenomena was first discovered more than 30 years ago in non-human primates, that were used as a model system to study eye movement (Robinson papers). Subsequently, similar homologous structures have been discovered in fishes, where a nuclei located in the hindbrain is responsible for velocity-to-position integration (VPNI) for eye movements. Similar neural responses to stimuli are observed in other tasks such as working-memory tasks (wang XJ , review), where we observe neurons that fire persistently, long after the termination of the initial stimulus. The mechanism by which groups of neurons perform such a task remain unknown.

In the cat prepositus nuceli, where similar integrator neurons reside, it was discovered that there were roughly three to four types of cells that were morphologically distinct (McCrea and Baker [1985]). There were principal cells, multi-dendritic cells and small cells, that had each unique morphology and axonal projections. The principal cells, were medium sized cells, importantly with ipsilaterally projecting axons that gave rise to local collaterals. Where as the multi-dendritic cells typically had complex dendritic patterns, with axonal projections that projected on the same side without any local collaterals. The small cells had dendritic fields similar to the principal cells, but with axons that crossed the midline. Similarly, in the goldfish brain stem, position sensitive cells were seen to be have similar morphologies, with ipsilaterally projecting cells having large dendritic fields with axons that gave rise to collaterals and contralateral projecting cells what did not have any ipsilateral projections and smaller dendritic fields (Aksay et al. [2000]). The emergence of axonal collaterals on the same side as other position sensitive cells, suggests the possibility of local feedback loops that migh drive this persistent activity. Supporting this evidence was also evidence that shows that pairs of neurons on the same side have highly coorelated activty, both in fish (Aksay et al. [2003]) and in monkeys (Dale and Cullen [2015]). For the eyes to have coordinated movement, there must exist mutual inhibiton between integrators on either side of the midline, which would presubambly be inhibitory in nature (Aksay et al. [2007]). These studies suggest that structural features of the circuits that perform this neural integration are likely similar across species, and that studies in one may be informative to the other (Joshua and Lisberger [2015]).

However, beyond this we do not know much about the detailed morphology of these cells, how many synapses do they have, who are their synaptic partners. We do not yet know if position sensitive cells synapses onto each other, although indirect evidence would suggest that they do (Aksay et al. [2003], Dale and Cullen [2015]). To answer some of these question, we chose to perform serial electron microscopy on postion sensitive cells in the hindbrain of larval zebrafish. The larval zebrafish is beleived to have ~100 integrator neurons unilateally, which makes such a system amenable to large scale imaging efforts, and that the organization of these cells in the larval animal migh most likely be conserved in the adult (Gilland et al. [2014]). This analysis reveled that the existance of atleast three groups of neurons that were part of the unilateral integrator. We found neurons with ipsilateral axons that gave rise to collaterals withing the same dendritic field as other integrator neurons. Apart from the previously know ipsilateral and contralalteral projections (Lee et al. [2015]), we found few neurons with both ipsi and contralaleral projections. Distributuon of synaptic locations of both pre and post synapses for all neurons revealed on average these cells recevied three time more input than output. We can extend the significance of these findings by inferring the neurotransmitter identity of these neurons based on the location of the cells bodies, as they are known to express glutamate and GABA in atternative stripe like patterns in the hindbrain (Kinkhabwala et al. [2011]). Doing so, suggests that the cells with ipsilaterally projecting axons and collaterals is excitatory, cells with contralatrally projecting axons are inhibitory. The remaining groups are presumably putative gutamatergic and glycenergic neurons. These results suggsest that the neural integration is acheived by positive excitatory feedback unilaterally, and by mutual inhibiton cont

## 2 Materials and Methods

Optical imaging. The optical imaging was performed using a custom built two photon microscope. Larval zebrafish that were 5-6 dpf were injected with calcium sensitive dye OGB by gently removing skin over the hindbrain and using a patch pipette for iontophoresis. The next day the animals were imaged on a 2photon microscope (wavelength). The animal was immobilized in

low melting agar and was positioned to view a monitor with light gratings. During spontaneous behavior, the hindbrain of the animal was imaged at predefined planes at ( image speed Hz). Once this was performed, the animal was anesthetized and the skin over the hindbrain was removed and the animal was immersed in fixative to preserve the ultrastructure.

#### Electron microscopy.

The optically imaged animals were immersed in a fixative of 1% paraformaldehyde and 1% glutaraldehyde buffered in 0.1M Cacodylate buffer for 24 hrs. Following which they were thoroughly washed in 0.1M Cacodylate buffer before staining. The tissue was stained using a conventional ROTO procedure [cite]. Following staining, the tissue was infiltrated with an EPON based resin for 24 hrs and baked for 48 hrs at 60C. The EPON based resin was tailored to be a low viscosity resin to help with better infiltration for this tissue. Following hardening, the tissue block face was coarsely trimmed and a rectangular mesa was defined for serial sectioning. Serial sections from the above animal were collected from the level of the Mauthner cell at a thickness of 45nm. The serial sections were collected similar to a method described here (Hayworth et al. [2014]). The serial sections were then adhered to a silicon wafer and imaged in a Zeiss field emitting scanning electron microscope using a custom software interface to collect the images (Hayworth et al. [2014]). The imaged volume was 200x150x60 um<sup>3</sup> (check final numbers). The images were montaged and aligned using the TrakEM2 plugin in Fiji(Cardona et al. [2012]).

#### Registration of 2P volume onto EM volume using TrakEM2

We first ID'ed potential VPNI cells from the LM dataset using methods that were previously described (Miri et al. [2011b]). To locate the same cells in the LM volume to the EM volume, we registered the two volumes using gross anatomical features like easily recognized clusters of cell bodies and blood vessels. This process was also performed in TrakEM2 (Cardona et al. [2012]) . This process resulted in overlaying the LM volume onto the EM volume. Once this was done, we were able to locate the VPNI cells in the EM volume.

#### Reconstructions

the reconstruction of the cells was performed using the TrakEM2 plugin in Fiji. Two expert tracers reconstructed the cells beginning from the cell bodies in an independent manner. The traces of the two tracers were then imported into Matlab using custom scripts and compared by a third reviewer. The third reviewer, independently reviewed points of disagreement and decided which trace was correct. In some cases, the traces were re-visited by the tracers if it was needed. During tracing, all pre and post synaptic sites were annotated. All traces were exported from TrakEM2 as \*.swc files and imported into Matlab using custom scripts. For the comparison of EM traces with LM traces, the LM traces were traced using the Simple Neurite Tracer (Longair et al. [2011]) plugin in Fiji, and exported as a \*.swc file.

#### Analysis

All analysis were performed using custom scripts written in Matlab.

## **3 Results**

The larval zebrafish has previously been established as a model system to study the hindbrain oculomotor integrator circuit, it offers the ability to optically record from multiple cells involved in the behavior due to its transparent body. It is also more invasively accessible as compared to more larger animal models like the non-human primate. In the current study, we looked to optically record from cells in the hindbrain of the larval zebrafish involved in the horizontal saccadic behavior, followed by

anatomically reconstructing the same cells participating in this behavior at the ultrastructure level.

The oculomotor integrator circuit has been a long standing question in neuroscience. Over the last 20 years studies have proposed various models that could act as integrators [cite]. One of the most simplest forms of a circuit, would be that of cells that are recurrently connected to each other, such that upon excitation, the signal is propagated to these recurrently connected cells feedback activity to give rise to a persistent 'loop' of activity. For such systems to exist, the weights of the recurrent synapses must be very precisely tuned and the relaxation times of excitation are typically assumed to be the same for all cells in the circuit (Seung [1996]). There also exist models that propose to perform integration without feedback, here the main assumptions are ..... (Goldman [2009]).

More recently, studies have predicted that there must be specific rules of connectivity among the cell of this circuit in oder for it to function the way it does. Other studies have show the evidence of common inputs to the cells in the VPNI (Dale and Cullen [2015]). Here we set out to understand the rules of connectivity between the velocity to position integrator (VPNI) cells in the larval zebrafish. To do this we have optically recorded from cells in the hindbrain of the larval zebrafish, followed by serial section electron microscopy of the same animal to reconstruct the VPNI cells from the previous step.

### **3.1 Registration of light microscope and electron microscope volumes ( figure 1)**

To determine the types of cells that were involved in the integrator network, we first imaged activity of cells in the hindbrain of the larval zebrafish. The larval zebrafish has been previously used as a model to study the oculomotor integrator circuit (Schoonheim et al. [2010], Miri et al. [2011b,a], Dale et al. [2015], Gonçalves et al. [2014], Lee et al. [2015]) and is believed to be similar to mammalian oculomotor circuits. To perform the functional imaging of these cells, the animal was previously electroporated with the calcium sensitive dye OGB in the hindbrain, using methods similar to (Aksay et al. [2007], Miri et al. [2011b]). Functional imaging was performed by placing the animal in an arena, with optical grating while imaging the hindbrain at predefined planes that was 8 microns apart ( fig 1A). The differential calcium traces were then converted to firing rates based in methods described previously (Miri et al. [2011b]). Once functional imaging of the animal was performed, the animal was immediately prepared for electron microscopy by immersing the animal in fixative. We chose to perform the light microscopy at planes close to the Mauthner cells, as this would later serve as a landmark to identify cells in the electron microscopy volume. The animal was processed for electron microscopy using conventional reduced osmium staining techniques and embedded in an EPON based resin. The tissue block was then coarsely trimmed until the appearance of the Mauthner cell plane. At this point, sections were collected in an automated manner using an automated tape collecting ultramicrotome (ATUM) as described previously (Hayworth et al. [2014]). The sections were then imaged in a field emitting scanning electron microscope (FE-SEM) to obtain an electron microscopy volume. In total for the EM volume we imaged, 15791 sections or  $\sim 10^{11}$  pixels ( fig 1B). These images were registered using the trakEM2 plugin in fiji (Cardona et al. [2012]). The images were first montaged using affine transforms followed by elastic transforms. Following this they were aligned in the z dimension, using affine and elastic transforms. In total, the light microscopy imaging volume was .... and the electron microscopy volume that was collected and imaged was .... ( fig 1b)).

To locate the cells that were involved in the VPNI circuit, we first identified cells in the light microscopic volume that were eye-position sensitive. Of these cells, a small fraction of cells, displayed behavior that was consistent with integrator cells. These cells had persistent firing, indicated by elevated calcium responses, long after the initial saccadic stimulus. Average

saccade triggered responses of these cells show cells with a range of persistence times. Cell with high persistence had long calcium decay time constants, where as leaky cells had shorter decay time constants ( fig 1D). Once these cells were located in the light microscopic volume, we looked at the LM stack to locate other morphological features that could be used to identify cells in the EM stack. First, we were able to locate some of the vasculature in low-resolution EM images. These locations were then used to precisely locate the same feature in the high resolution EM images, with a small window, as compared to searching for these features in the high-res images itself. Once enough such features were identified, we used these landmarks to calculate an an affine transform that overlaid the LM volume on the EM volume using the TrakEM2 plugin in Fiji (Cardona et al. [2012]). Once this was done, we were able to ID all cells with position signal from the LM and EM volumes. In total, we were able to indetify 22 cells with eye-position sensitive signals they also displayed integrator like behavior. Although these cells were from three predefined planes in the LM volume, the centers of the cells identified in the EM volume put them in multiple planes. The cells were located in rhombomeres 7/8 of the larval zebrafish. We were also able to identify anatomical landmarks like the contralateral Mauthner cell axon, which is clearly visible in the the EM volume. All cells in this volume were lateral to the contralateral Mauthner cell axons, and the centroids of the cells around the centroid of the Mauthner cells. Similarly, other anatomical landmarks like the commissures are also visible in the EM dataset ( fig 1E). Registration of the LM volume to the EM volume revealed the location of 22 VPNI cells. Although the cells were from three planes in the light microscopic volume, their annotations in the EM volume was not necessarily restricted to three distinct planes, since we annotated the centers of the cells in the EM volume. The cells spanned 23  $\mu$ m in the dorsoventral axis.

### 3.2 Morphology and axonal projection patterns of registered VPNI cells ( figure 2)

Not much is know about the morphology of cells that are involved in the VPNI circuit. Previously dye fills in the goldfish area1, established the role of eye-position sensitive neurons in VPNI behavior, this study also revealed that there were at least cells with 2 types of axonal projection, those that were ipsilateral and those that were contralateral (Aksay et al. [2000]). More recently, in the larval zebrafish VPNI system, it was reported that there were at least classes of cells that projected either ipsilaterally and were excitatory or projected contra laterally and were withe excitatory or inhibitory. Here we aimed to build on this body of work by characterizing the ultrastructure of cells belonging to these classes. Of the VPNI cells that were reconstructed, there were 7 cells (31%) that had a clear distinguishable axon, with the presence of presynaptic sites on their neurites. Of the remaining cells, 8 cells (36%) had putative axon-like neurites that crossed the midline in a very stereotypic pattern. The remaining 7 cells, did not have any distinguishable neurites that were axonal in nature. All cells had neurites that we dendritic in nature, they were identified by the presence of postsynaptic sites that were studded along the neurite. In total, we reconstructed 22 cells from xxxx cells in the imaged volume, containing 9.5mm of neurite, 406 presynaptic sites and 2229 postsynaptic sites. On average a cell had  $101.31 \pm 74.15$  postsynaptic sites and cells thad had axons had  $58 \pm 44.39$  presynaptic sites.

#### Somata

The cells were reconstructed form the soma outward. Typically, we observed that somata gave rise to neurites that were ventral to the location the somata. We observe a consistent darkening of the membrane with intermediate gaps over multiple serial-sections along the somal mebrane that resembled gap junctions (sup figure), consistent with evidence in the developing larval

zebrafish there exists gap junctions in the rhobomeres (Jabeen and Thirumalai [2013]). However, the resolution of our imaging setup makes it hard to distinguish gap junctions as the classical pentameric structure that is readily observed in the TEM. In most cases the neurite that emerged from the cell soma were of constant diameter (sup figure), with no discernible trend of whether a neurite was axonal or dendritic in nature. We observed on average  $3.3 \pm 1.5$  (mean $\pm$ std) neurites that emerged from the somata of the VPNI cells. An interesting feature that was observed in all of the cells was the presence of a neurite that was enriched with microtubules, that typically projected  $<1\mu\text{m}$  from the cell body. In some cases, this neurite terminated inside glial like processes, but these neurites were devoid of any features other than microtubules. The purpose of this neurite remains unknown. In general we also observed that the neurites almost always projected ventral to the cell somata, with a few exceptions. The spatial location of the VPNI cells ended up in three broad clusters, there was one cluster of cells that was located very close to the midline and very rostral in the imaged volume. Similarly, there was a tight cluster of cells that was located at the caudal extent of the imaged volume, and a third loose cluster of cells that was located at the lateral most extent of the volume, with cells that spanned over the rostrocaudal range (figure). It must be noted that the calcium dye was loaded approximately in between the second and third clusters at a caudal location. We also observed that the spatial locations of the first cluster of cells was intermingled with the commissure bundles, close to the contralateral Mauthner axon.

### **VPNI cells have specific axonal projection patterns ( figure 3)**

In the past it was shown that neurons from in the hindbrain of the larval zebrafish, have a striking organization in neurotransmitter identity, based on the type of cells, its morphology and projection patterns (?). It was observed that the VPNI cells in the hindbrain comprised of at least 3 classes of these cells (Lee et al. [2015]), where the classes of cells corresponded with stereotypic axonal projection patterns. These classes were either glutamatergic or GABAergic in their neurotransmitter identity. However, in previous studies, axons were identified from light microscopic images of VPNI cells that were dye filled, and was inferred based on the thickness of the neurite (confirm). However, the real identity of the axon can be confirmed by the presence of presynaptic terminals along the neurite, which is possible to observe from ultrastructural images. Thus, axons were defined as those neurites that were identified by the presence of presynaptic sites along the neurite (figure). We also observed that axons typically consisted of a long shaft that gave rise to collaterals along the length of the shaft. We also noticed some of the the neurites that were reconstructed, to be very ‘bare’, with no pre or postsynaptic terminal on them. These neurites in all cases projected to the contralateral side, and were typically engulfed by glial like processes just before the midline crossing. It is known that in the larval zebrafish, there exists astrocytes that are expressed along the midline that form a ‘glial bridge’ that are necessary for axon guidance (Barresi et al. [2005]). Since, these glial-bridges are involved primarily in axonal guidance, they process before crossing the midline were considered putative-axons. During the course of reconstruction, we also noticed that the VPNI neurons had specific axonal projection patterns. Thus, for the remainder of this study, we term these neurites, that do not have any postsynaptic termination, and that are engulfed by glia, to be putative-axons (figure). Following the annotation of neurites as axonal, we divided the cells in the VPNI population into four groups based on their axonal projection patterns as (i) ipsilaterally projecting (ii) contralaterally projecting (iii) Ipsi and contra projecting (iv) unknown.

Ipsilaterally projecting (group1) - Of the cells, 6 cells ( $n=6/22$  cells) were observed to have purely ipsilaterally projecting axons. Figure 3, panel A shows all 6 cells where the dendrites are axons are labeled with lines of different thickness. The axons were clearly identified by the presence of en passant boutons and presynaptic vesicle clouds all along the neurite. The

cell bodies of these cells were located at the rostral extent of the volume, and close to the midline. The axons of these cells extended along the rostrocaudal axis with tilt in the dorsoventral axis. Typically the caudal segment of the axon was more dorsal as compared to the rostral segment of the axon, following the body outline of the animal. We noticed that these axons gave rise to collaterals that extended along the mediolateral axis. The rostral segment of the axon extended toward the abducens nuclei, which contains the motor neurons that innervate the eye muscles. The caudal segment extended further into the hindbrain where they presumably synapse onto other cells in the rhombomeres. The axons of these cells in general were the longest, which is not surprising as the imaged volume was from the ipsilateral side only. An interesting observation that we made was the neurites that were identified as axonal, did not necessarily begin with being axonal. In fact in most cases, these neurites contained many postsynaptic sites similar to dendrites, before the emergence of presynaptic sites (arrow head in figure 2). We also observed that in one case, the axon of the cell was myelinated along the rostrocaudal section of the axon (figure 2A). The myelination was not present uniformly throughout the axon, but along small segments of the axon. In each case, the myelination terminated briefly for a collateral, to subsequently resume myelination. Similar myelin sheaths have been previously seen in zebrafish spinal cord neurons and are thought to wrap these cells in an activity dependent manner (Mensch et al. [2015], Hines et al. [2015]). The average length of the axons from these cells was  $270.05 \pm 244.06$   $\mu\text{m}$  with the longest reconstructed axon being  $683.39$   $\mu\text{m}$ . Similarly, we also measured the diameter of the axons from these cells. The diameter of the axons from these cells was on average  $0.20 \pm 0.15$   $\mu\text{m}$  with lognormal like distribution of the diameter along various segments of the axons (sup figure).

Dendrites of cells in this group extended laterally from the cell somata and were always ventral to the cell somata. Dendrites arborized over a large area with the dendritic fields of these cells overlapping with each other. The dendrites were also found to be distributed over the dorsoventral axis with peak arborization at  $35.6 \pm 8.4$   $\mu\text{m}$  ventral to the cell somata respectively. The axonal diameter distribution was significantly different as compared to the dendritic diameter ( $p < 1e-5$ , Kolmogorov-Smirnov test), and the average axonal diameter of these cells was significantly smaller as compared to the average diameter of the dendrite ( $p < 0.05$ , t-test).

Ipsi and contra projecting (group 2)- A handful of cells ( $n=2/22$  cells) had axons with two projections. These cells were located lateral to the cells in group 1 and the average length of these cells were as long as cells in group 1. One of the two axons was found on the ipsilateral side with en passant boutons containing presynaptic sites with vesicle clouds opposing postsynaptic densities. This axon was similar to the ipsilaterally projecting axons that were previously noticed in group 1. In general the length of the axon was similar in length to the axons from group 1. These cells contained another projection that was not obviously axonal or dendritic. We termed these midline crossing neurites as putative-axons due to some of the features that are shared with ipsilaterally projecting axons and developmental features. The first of these features is the fact these neurites were 'bare' for the most part, similar to some of the initial axonal segments of ipsilaterally projecting neurites where there were no presynaptic terminals. Second, they were engulfed by glial like processes, just before crossing the midline, consistent with the idea of glial-bridges that are instrumental in axonal guidance during development (Barresi et al. [2005]). And thirdly, the diameter of these neurites was similar to diameter of axons on the ipsilateral side as compared to the diameter of dendrites (sup figure). Due to these three criterion, we termed these midline crossing neurites as putative-axons.

The dendrites of these cells were of similar length to the dendrites as the cells from group 1 and spanned a similar range.

Contralaterally projecting (group 3)- The cells located at the caudal most extent ( $n=8/22$  cells) of the imaged volume contained

exclusively contralaterally projecting putative-axons. In all examples of cells in this group, we observed that the neurite that crossed the midline was a putative-axon. Although we did not observe any direct presynaptic terminals on any of the neurites, we observed that the neurites that crossed the midline satisfied the three criteria that we used to check if they were putative-axons. These neurites were bare, with no synaptic terminals, they were engulfed by glia just before crossing the midline and the diameter of these neurites were significantly smaller to the diameter of the dendrites ( $p = 9.9765e-05$ , ttest). The axonal diameter distribution was also significantly different as compared to the dendritic diameter distribution ( $p < 1e-04$ , Kolmogorov-Simironov test). Unlike the previous groups of cells, the axons of these cells typically emerged from the somata of the cell, and crossed the midline at locations ventral to the cells somata. In some cases it was noticed that a collaterals emerged from these neurites, but they were dendritic in nature (figure). The dendrite from cells belonging to this group, on average were  $292.41 \pm 69.75 \mu\text{m}$  in length. This was significantly shorter as compared the dendrite from group1, whose average length was  $391.83 \pm 65.83 \mu\text{m}$  ( $p < 0.05$ , ttest). In all cases, the dendrite form all cells, terminated within the imaged volume. The dendrites of cells, arborized over a much smaller area as compared to the dendrites from group1. The dendrites of this group of cells tended to arborize very close to their cell somata, the peak arborization was at  $8.6 \pm 7.3 \mu\text{m}$  from the cells somata, which is significantly more dorsal as compared to cells form group 1 (ttest,  $p < 1e-04$ ).

Unknown projecting (group4) - The last group of cells ( $n=7/22$ ) were located at the lateral most extent of the volume. These cells had no identifiable axon based on the three criterion that we have used so far. We believe this is most likely because these cells were not fully represented in the imaged volume and neurites of these cells exit the volume before the axon was located. The dendrites of the cells in all cases extended medially in the imaged volume, but to varying extents. In some cases, the dendrites extended medially, at locations very close to the cell somata, whereas in other cases, the dendrites extended medially, but gradually along the rostrocaudal extent of the volume. The average length of the dendrites for cells from this group was  $221.47 \pm 48.70 \mu\text{m}$ , which was not significantly different compared the the length of the dendrites from group3 cells. The dendrites of these cells were significantly smaller as compared to the dendrite from cells in group1 ( $p < 1e-3$ , ttest).

### 3.3 Distribution of synapses on VPNI cells ( figure 4)

The synaptic distribution of all VPNI cells in this imaged volume was obtained as a result of reconstruction and annotation of all pre and postsynaptic sites. Our imaging resolution of 5nm/pixel gave us the ability to annotate all synapses very accurately. We were able to identify synapses with the presence of vesicle pools and an opposing postsynaptic density darkening for all annotated synapses in this volume. To our knowledge nothing is known about the synaptic distribution of cells in the zebrafish hindbrain. The most widely studied cell in the hindbrain, at the level of ultrastructure is the Mauthner cell. In general during the annotation, we labeled those sites as synaptic that had a pool of vesicles opposed to a dark postsynaptic density. We did not label synapses as being either symmetric or asymmetric, to infer neurotransmitter identity, as this is not precise (Klemann and Roubos [2011]).

Since our imaged volume was unilateral, we looked at the possibility of cells in group1 and group2 to be in the best position to form functional synapses with other cells. But in order to infer any results from any of these reconstructions, we checked to see if the axons of these cells were of similar length compared to previous efforts, where VPNI cells were dye filled and imaged, in order to reconstruct their morphologies. Of importance was the extent to which the collaterals of the axons of these cells matched. We compared the number of collaterals and he length of these collaterals from ipsilaterally projecting VPNI cells that

were reconstructed from the EM volume, to cells that were dye filled. In both cases, the collateral lengths and the number of collaterals, there was no significant difference between ipsilaterally projecting VPNI cells (figure 3).

group1 neurons: Cells in group1, with ipsilaterally projecting axons, had, on average, the largest number of both pre and postsynaptic sites. On average, cells in this group contained  $174.83 \pm 88.09$  postsynaptic sites, and  $56.5 \pm 52.75$  presynaptic sites. The distribution of the synapses on these cells were also analyzed. We found that the average pathlength of postsynaptic sites was  $237.82 \pm 133.08$   $\mu\text{m}$  from the cell soma, whereas the mean presynaptic pathlength was  $618.43 \pm 208.29$   $\mu\text{m}$  from the cell soma. Cells tend have postsynaptic sites close to the cell somata, whereas presynaptic sites that were at least  $\sim 150$   $\mu\text{m}$  away from the cell somata.

group2 neurons: Cells in group 2 had an ipsilaterally projecting axon and a putative contralateral projecting axon. These neurons on an average have  $126.5 \pm 70$  postsynaptic sites, similar to the number of postsynaptic sites on group1. This is also evident by the fact that the length of the dendrites of group1 and group2 were similar, however, the distribution of the synapses on these two groups differed. There was a significant difference in the distribution of postsynaptic sites onto cells from group1 as compared to cells from group2 ( $p < 0.05$ , Kolmogorov-Smirnov test). Similarly, these cells had on average  $33.5 \pm 7.77$  presynaptic sites on their ipsilaterally projecting axon.

group3 neurons: The dendrites of these cells were completely encompassed in the imaged volume. On average, these cells had  $85.2 \pm 39.5$  postsynaptic sites. The distribution of the pathlengths of postsynaptic sites on these cells were significantly different as compared to the distribution on cells from group1 and group2 ( $p < 1e-10, p < 1e-4$  respectively).

group4 neurons: Lastly the group4 neurons that were located at the lateral most extent of the volume had on average  $40.83 \pm 25.11$  postsynaptic sites.

#### intersynaptic distance:

Next we looked at the intersynaptic distance for all pre and postsynaptic sites. In general we found that these distance followed a lognormal distribution, much like many other parameters in the mammalian brain. The mean interpostsynaptic distance was  $1.69$   $\mu\text{m}$  and the mean interpresynaptic distance was  $1.93$   $\mu\text{m}$ .

### **3.4 VPNI cell to cell connectivity ( figure 5)**

It is yet to be determined if integrator cells synapses onto each other. Presumably for VPNI cells to synapse onto each other, the axons of some of these cells must come in close contact to the dendrites of other cells. We looked at the minimum distance between cells with axons (presynaptic cells) and cells with dendrites (postsynapse). In Figure 5B, we plotted the minimum distance between cells with axons and corresponding cells with dendrites. Here we noticed that of the 7 cells with axons that had presynaptic sites, only 2 of these cells had distances that were in the range that was permissible to make synapses. We next look only at those axon-dendrite pairs that were within  $1\mu\text{m}$  of each other. Of the 8 sites that were within a micron of each other, 4 of these sites were actual synapse. All 4 synapses emerged from one cell in this imaged volume. This one cell belonged to group1, with ipsilaterally projecting axons. This cell makes 2 synapses onto another group1 cells and 1 synapse each onto two group 3, contralaterally projecting cells. This is the first demonstration that cells that take part in the velocity to position integration are indeed monosynaptically connected to each other. These synapses also lie on the axons collaterals of the cell that makes the synapses. We also observed that all the synapses were within  $1\mu\text{m}$  of an axon that came in contact with a dendrite, and that only this one cell, was in a position to make synapses onto other cells, as many of its axonal nodes

were within 1um of the dendrites of the other cells. Translating these presynaptic cells within the volume, did not reveal any significant increase in the number of contacts between cells, suggesting that this one cells was well poised to makes synapses onto other cells, and that the remaining presynaptic cells did not share much of an overlap with the dendrites to form functional synapses ( sup fig).

## 4 Discussion

The aim of this work was to see if it was possible to combine functional imaging of a subset of neurons and detailed morphological reconstructions of the same neurons in order to understand the working of the overall circuit. Here we report that we were able to successfully register an light microscopic functional volume to its corresponding serial sectioned imaged volume. Reconstruction of the neurons that were involved in the VPNI task revealed that the circuit comprised of at least 4 distinct groups of cells based on their axonal projections and synaptic distributions. Ipsilaterally projecting cells for which both axon and dendrite were present, had at least 3 inputs synapses for every output synapses. The reconstructions also validated a long standing question in systems neuroscience and showed that VPNI cells synapse onto each other, specifically, the ipsilaterally projecting cell synapses on other ipsilateral and contralateral projecting cells. Put together, these results suggest the detailed organization of the VPNI system and provide hard numbers that can be useful to the broader neuroscience community as a resource to build accurate models of the integrator circuit.

Recent advances in high-throughput imaging technologies, have provided opportunities to visit long standing question in system neuroscience, here we re-visit one such long-standing question, that of the velocity-to-position-neural integrator. The eye-position neural integrator is located is the homologous structures located in the hindbrain of most mammals and vertebrates. Historically, this system was first discovered in monkeys (cite), where a nuclei, located deep in the hindbrain, the nucleus prepositus. However, as with all large animal studies, they do not have the numerous cellular tools that are available to systematically correlate function to structure. More recently, it was discovered that similar function was observed in the brain stem of gold fish (Baker papers) and subsequently in larval zebrafish ( Aksay paper,Baier paper, Engert paper). Here we use the larval zebrafish as a model system to understand the functional architecture of a system that is involved in this task. The larval zebrafish is conducive to optical imaging as it is transparent during the larval stages, and it is thought that there are ~100 cells unilaterally ( source) in the hindbrain that are involved in the VPNI task. Inferring functional connectivity by serial electron microscopy was important in this system as the larval zebrafish proves to be hard to perform paired patch recordings. And if the number of functional synapses between any two integrator cells are very few in number, this task is every more hard. However, performing serial electron microscopy of registered cells allows the direct visualization of functional synapses between these cells. It is also possible to observe other non-conventional forms of synaptic communication, like dendro-dendritic, axo-axonal and electrical synapses using serial electron microscopy.

Larval zebrafish neurons in the hindbrain were loaded with calcium sensitive dye, following which these neurons were functionally imaged while the animals made spontaneous saccades. The same animal was then processed for serial electron microscopy. This process revealed the existence of three unique groups of cells, based on their axonal projections, with the fourth group of partially reconstructed cells. These groups, all had unique distributions of inputs ( postsynapses) on their dendrites.

The neurons of group1 were located rostrally and at medial locations. They had long ipsilaterally projecting axons and large dendritic arbors that extended laterally. These cells were also observed to have the largest fraction of both pre and postsynaptic sites. Cells in group2

- First demonstration of number of inputs to a VPNI cell
- Something about effect of distance on the function
- Ratio of inputs/outputs
- stripe inference

It is yet to be determined how many cells encode for eye-position sensitive signals in the larval zebrafish. Previous models of the integrator, both in monkeys and in zebrafish ( lisberger, miri) have suggested networks with strong feed forward connectivity and weak feedback connectivity.

- to be determined, who are the cells that are talking to VPNI cells
- what fraction of these cells are other ipsi, contra, dual cells
- what fraction of these are excitatory, and what fraction of these are inhibitory

## References

- E Aksay, R Baker, H S Seung, and D W Tank. Anatomy and Discharge Properties of Pre-Motor Neurons in the Goldfish Medulla That Have Eye-Position Signals During Fixations. *Journal of Neurophysiology*, 84(2):1035–1049, August 2000.
- Emre Aksay, Robert Baker, H Sebastian Seung, and David W Tank. Correlated discharge among cell pairs within the oculomotor horizontal velocity-to-position integrator. *The Journal of neuroscience : the official journal of the Society for Neuroscience*, 23(34):10852–10858, November 2003.
- Emre Aksay, Itsaso Olasagasti, Brett D Mensh, Robert Baker, Mark S Goldman, and David W Tank. Functional dissection of circuitry in a neural integrator. *Nature neuroscience*, 10(4):494–504, April 2007.
- Michael J F Barresi, Lara D Hutson, Chi-Bin Chien, and Rolf O Karlstrom. Hedgehog regulated Slit expression determines commissure and glial cell position in the zebrafish forebrain. *Development (Cambridge, England)*, 132(16):3643–3656, August 2005.
- Albert Cardona, Stephan Saalfeld, Johannes Schindelin, Ignacio Arganda-Carreras, Stephan Preibisch, Mark Longair, Pavel Tomancak, Volker Hartenstein, and Rodney J Douglas. TrakEM2 software for neural circuit reconstruction. *PLoS ONE*, 7(6):e38011, 2012.
- Kayvon Daie, Mark S Goldman, and Emre R F Aksay. Spatial patterns of persistent neural activity vary with the behavioral context of short-term memory. *Neuron*, 85(4):847–860, February 2015.

Alexis Dale and Kathleen E Cullen. Local Population Synchrony and the Encoding of Eye Position in the Primate Neural Integrator. *The journal of neuroscience*, 35(10):4287–4295, March 2015.

E Gilland, H Straka, T w Wong, R Baker, and S j Zottoli. A hindbrain segmental scaffold specifying neuronal location in the adult goldfish, *Carassius auratus*. *Journal of Comparative Neurology*, 522(10):2446–2464, July 2014.

Mark S Goldman. Memory without feedback in a neural network. *Neuron*, 61(4):621–634, February 2009.

P J Gonçalves, A B Arrenberg, B Hablitzel, H Baier, and C K Machens. Optogenetic perturbations reveal the dynamics of an oculomotor integrator. *Frontiers in Neural Circuits*, 8, 2014.

Kenneth J Hayworth, Josh L Morgan, Richard Schalek, Daniel R Berger, David G C Hildebrand, and Jeff W Lichtman. Imaging ATUM ultrathin section libraries with WaferMapper: a multi-scale approach to EM reconstruction of neural circuits. *Frontiers in Neural Circuits*, 8:68, 2014.

Jacob H Hines, Andrew M Ravanelli, Rani Schwindt, Ethan K Scott, and Bruce Appel. Neuronal activity biases axon selection for myelination in vivo. *Nature neuroscience*, 18(5):683–689, May 2015.

Shaista Jabeen and Vatsala Thirumalai. Distribution of the gap junction protein connexin 35 in the central nervous system of developing zebrafish larvae. *Frontiers in Neural Circuits*, 7:91, 2013.

M Joshua and S G Lisberger. A tale of two species: Neural integration in zebrafish and monkeys. *Neuroscience*, 296:80–91, June 2015.

Amina Kinkhabwala, Michael Riley, Minoru Koyama, Joost Monen, Chie Satou, Yukiko Kimura, Shin-Ichi Higashijima, and Joseph Fetcho. A structural and functional ground plan for neurons in the hindbrain of zebrafish. *Proceedings of the National Academy of Sciences of the United States of America*, 108(3):1164–1169, January 2011.

Cornelius J H M Klemann and Eric W Roubos. The gray area between synapse structure and function-Gray's synapse types I and II revisited. *Synapse*, 65(11):1222–1230, June 2011.

Melanie M Lee, Aristides B Arrenberg, and Emre R F Aksay. A Structural and Genotypic Scaffold Underlying Temporal Integration. *The journal of neuroscience*, 35(20):7903–7920, May 2015.

Mark H Longair, Dean A Baker, and J Douglas Armstrong. Simple Neurite Tracer: open source software for reconstruction, visualization and analysis of neuronal processes. *Bioinformatics*, 27(17):2453–2454, September 2011.

R A McCrea and R Baker. Cytology and intrinsic organization of the perihypoglossal nuclei in the cat. *The Journal of comparative neurology*, 237(3):360–376, July 1985.

Sigrid Mensch, Marion Baraban, Rafael Almeida, Tim Czopka, Jessica Ausborn, Abdeljabbar El Manira, and David A Lyons. Synaptic vesicle release regulates myelin sheath number of individual oligodendrocytes in vivo. *Nature neuroscience*, 18(5):628–630, May 2015.

Andrew Miri, Kayvon Daie, Aristides B Arrenberg, Herwig Baier, Emre Aksay, and David W Tank. Spatial gradients and multidimensional dynamics in a neural integrator circuit. *Nature neuroscience*, 14(9):1150–1159, September 2011a.

Andrew Miri, Kayvon Daie, Rebecca D Burdine, Emre Aksay, and David W Tank. Regression-Based Identification of Behavior-Encoding Neurons During Large-Scale Optical Imaging of Neural Activity at Cellular Resolution. *Journal of Neurophysiology*, 105(2):964–980, February 2011b.

Peter J Schoonheim, Aristides B Arrenberg, Filippo Del Bene, and Herwig Baier. Optogenetic localization and genetic perturbation of saccade-generating neurons in zebrafish. *The Journal of neuroscience : the official journal of the Society for Neuroscience*, 30(20):7111–7120, May 2010.

H S Seung. How the brain keeps the eyes still. *Proc. Natl. Acad. Sci. USA*, 93(23):13339–13344, 1996.

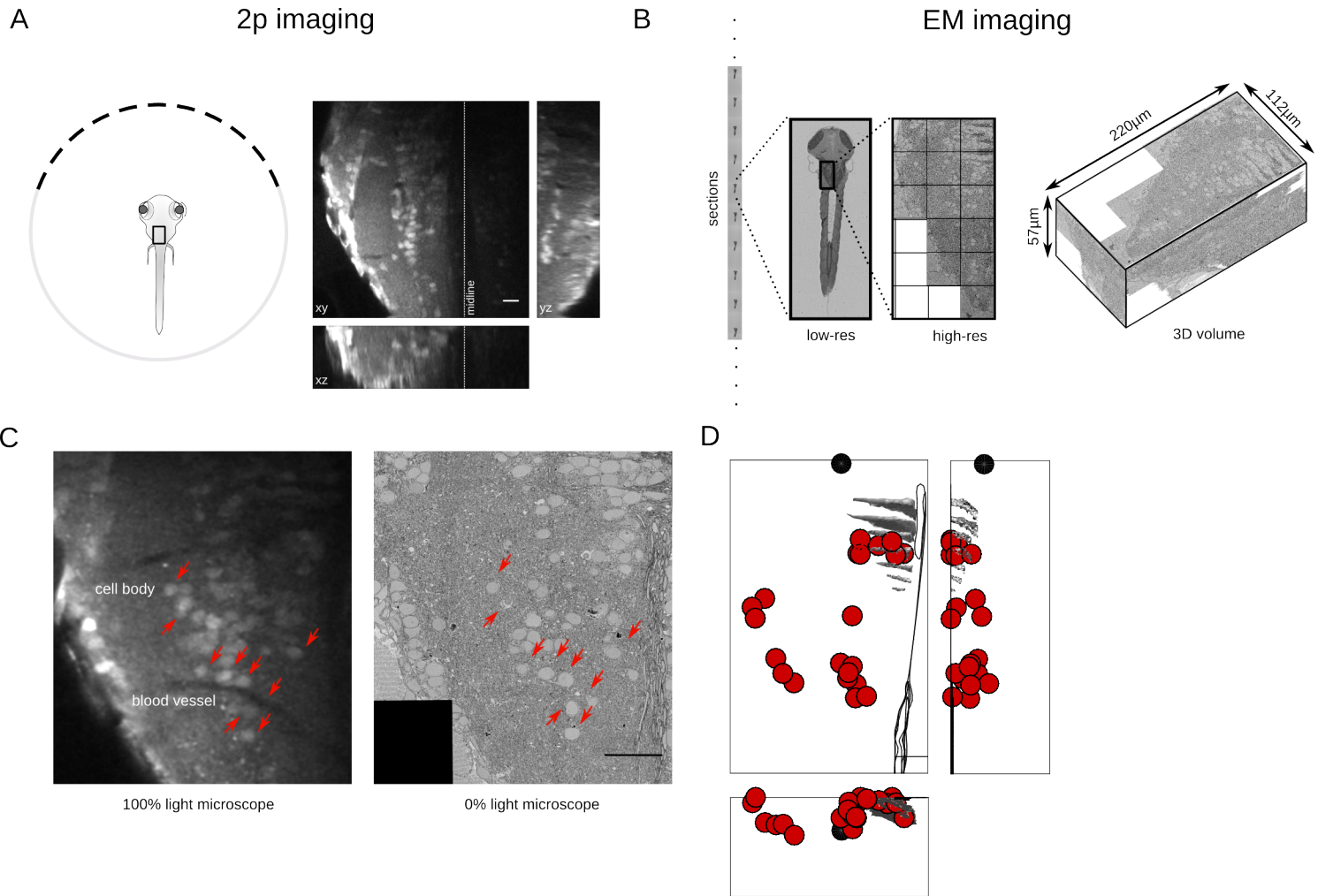


Figure 1: Registration of functionally imaged larval zebrafish to serial electron microscope images. (A) Schematic of the experimental setup with an example of the functional data that is obtained from two-photon light microscopy of calcium dye, during saccadic behavior. (B) Serial electron microscopy of same zebrafish from A, sections are collected on tape in an automated manner, images at low-res are used to align the sections, followed by images at high-resolution over the region of interest. 3D volume of the imaged area. (C) Registration of LM volume to EM volume to locate the cells that were involved in the behavior. Arrows indicate the same features in both LM and EM. (D) Anatomical location of all cell bodies involved in the behavior along with anatomical landmarks from the EM volume. (E) Functional data showing the average saccadic response for all cells.

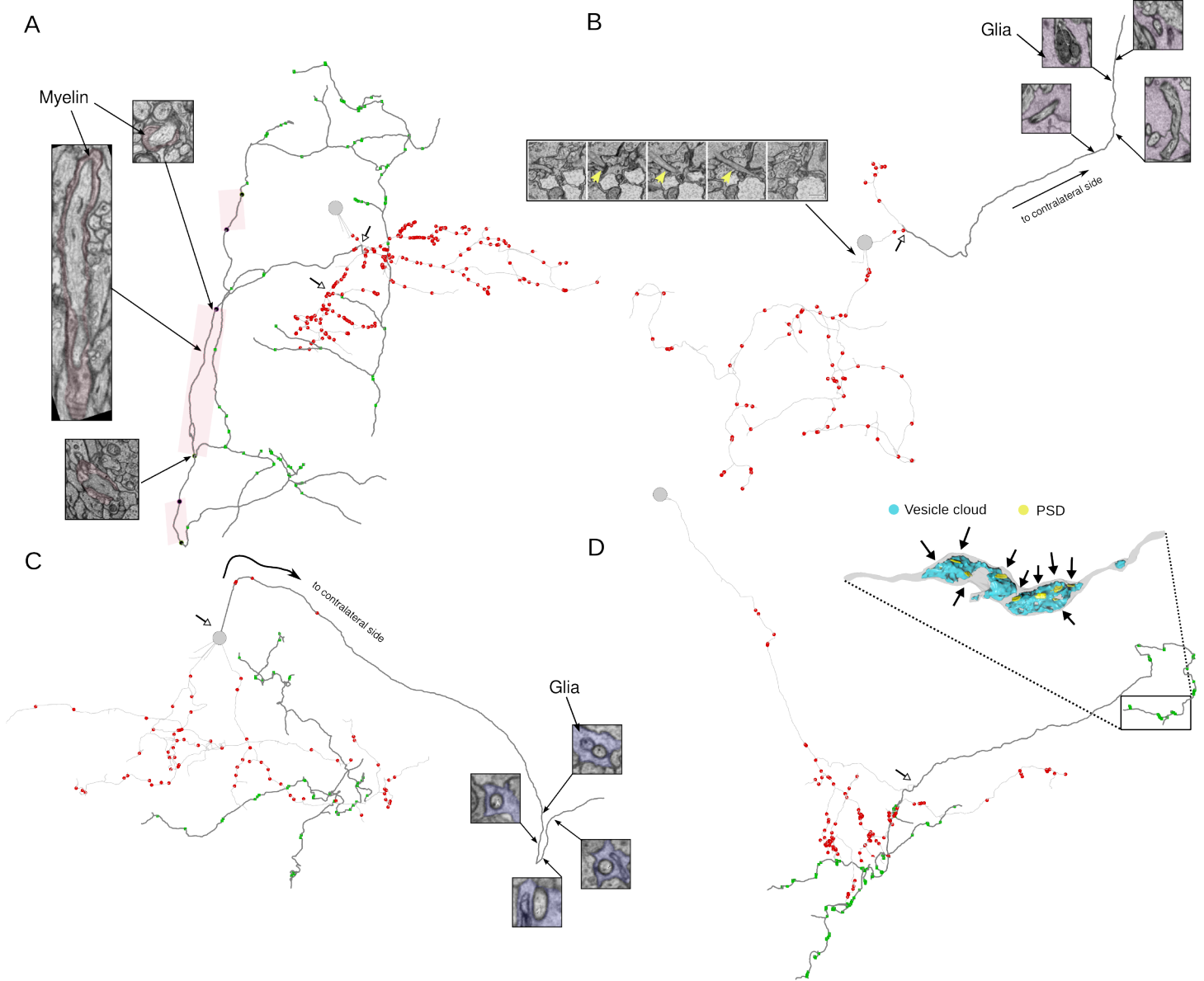


Figure 2: VPNI cell anatomical features, reconstructed from EM volume. (A) Example of VPNI cell showing axon (dark segments) and dendrite (light segments) with pre and postsynaptic locations. Parts of the axon of this VPNI cell are myelinated. Insets, (black dots) show the start, middle and the end of a myelinated segment of the axon. Other myelinated segments are highlighted in the colored box. Open arrow heads show the location of axon initiation zones along the neurite. (B) Example VPNI cell with putative-axon that is engulfed by glial processes before crossing the midline (inset right- colored segments are glial). Microtubule rich neurite that emerges from cell somata show in left inset. (C) VPNI cells with putative-axon that is engulfed by glia before midline crossing (right inset). Ipsilateral axon and dendrite also present for this VPNI cell. (D) VPNI cells with single neurite that branches to give rise to axon and dendrites. Axon is studded with presynaptic sites that are clustered along neurite. Inset is a 3D reconstruction of axon termination zone with large vesicle cloud with multiple post synaptic densities opposed to the vesicles.

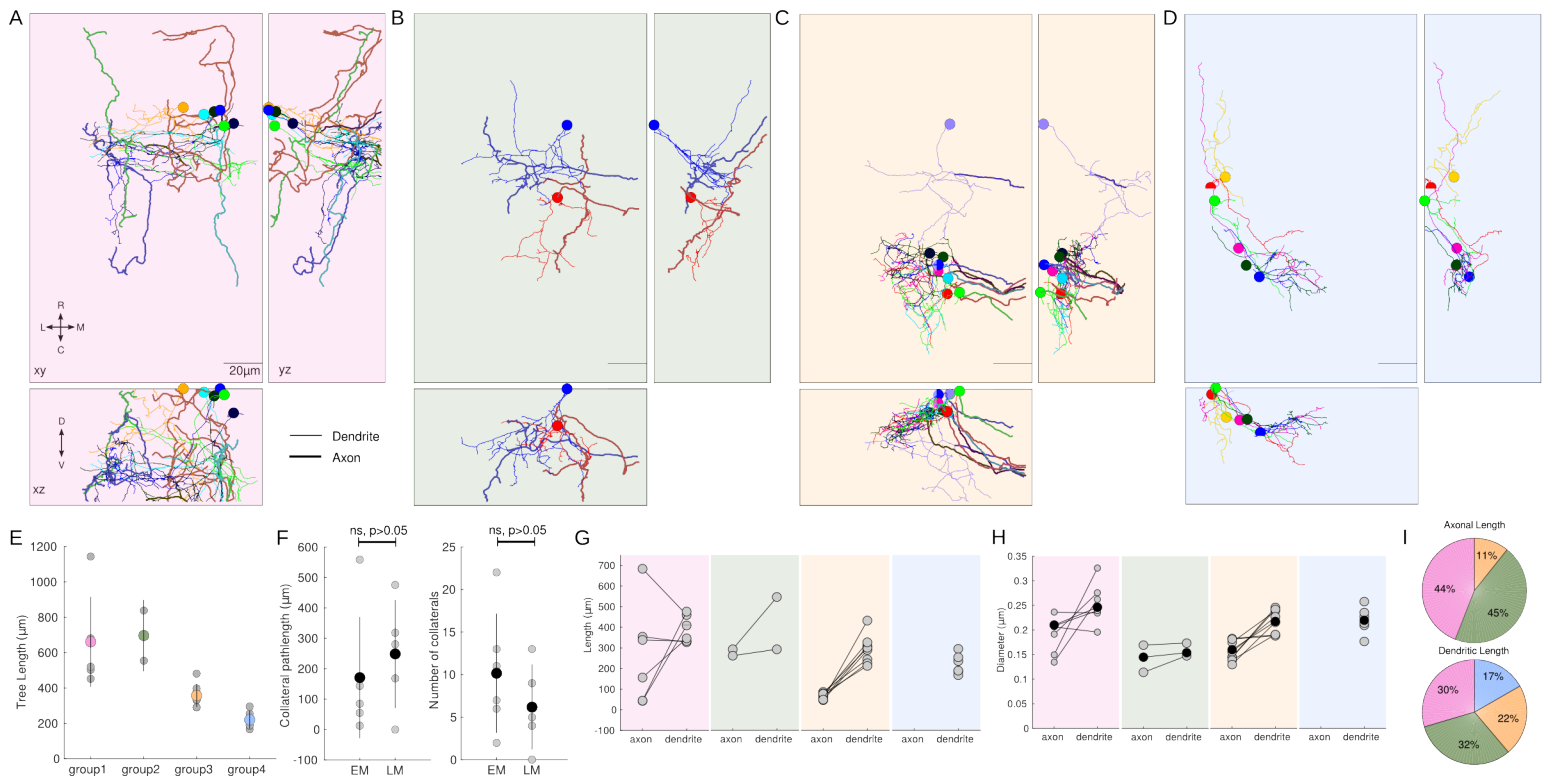


Figure 3: VPNI cells with distinct axonal projection patterns. (A) VPNI cell with ipsilateral projecting axons- group1. (B) VPNI cells with ipsilaterally projection axons and midline crossing putative-axon – group2. (C) VPNI cells with midline crossing putative-axon – group3. (D) VPNI cells with unknown axonal projection – group4. (E) Average tree length of integrator neurons from each group. (F) Number and length of axonal collaterals for ipsilaterally projecting axons reconstructed from EM and dye fill LM volumes. (G) Range of axonal and dendritic lengths for each group. (H) Average diameter of axon and dendrite for each group. Scale bar is 20um.

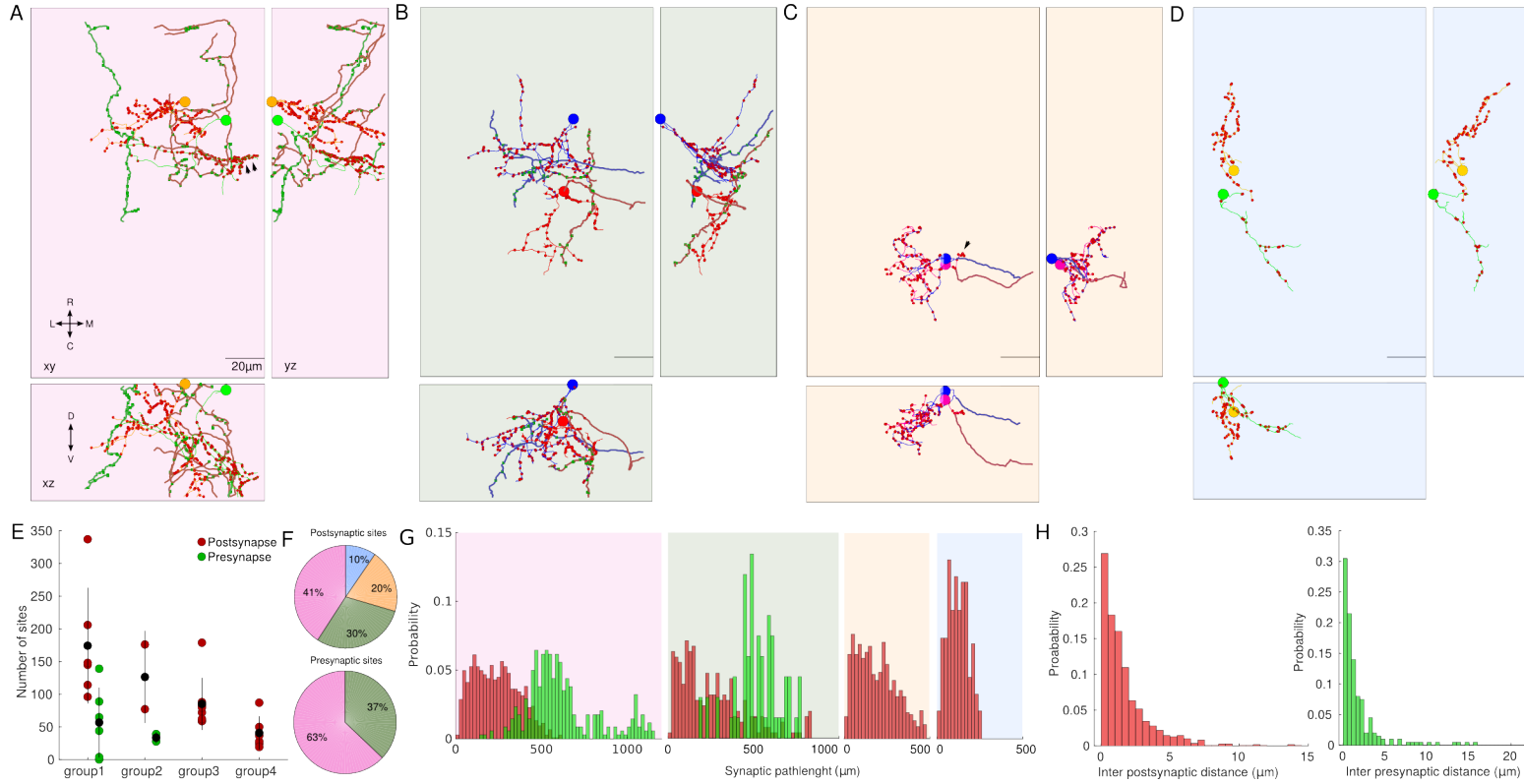


Figure 4: Synaptic distributions for VPNI cell groups. (A) Two representative VPNI cells with ipsilaterally projecting axons along with pre and postsynaptic sites. (B) VPNI cell with ipsilateral axon and contralateral putative axon. (C) Cells with contralateral putative-axon. (D) cells with unknown axonal projections. (E) Average number of synapses for each group. (F) Fraction of pre and postsynapses from each group. (G) Distribution of pre and postsynaptic path-lengths for each group. (H) Distribution of inter-post and presynaptic sites.

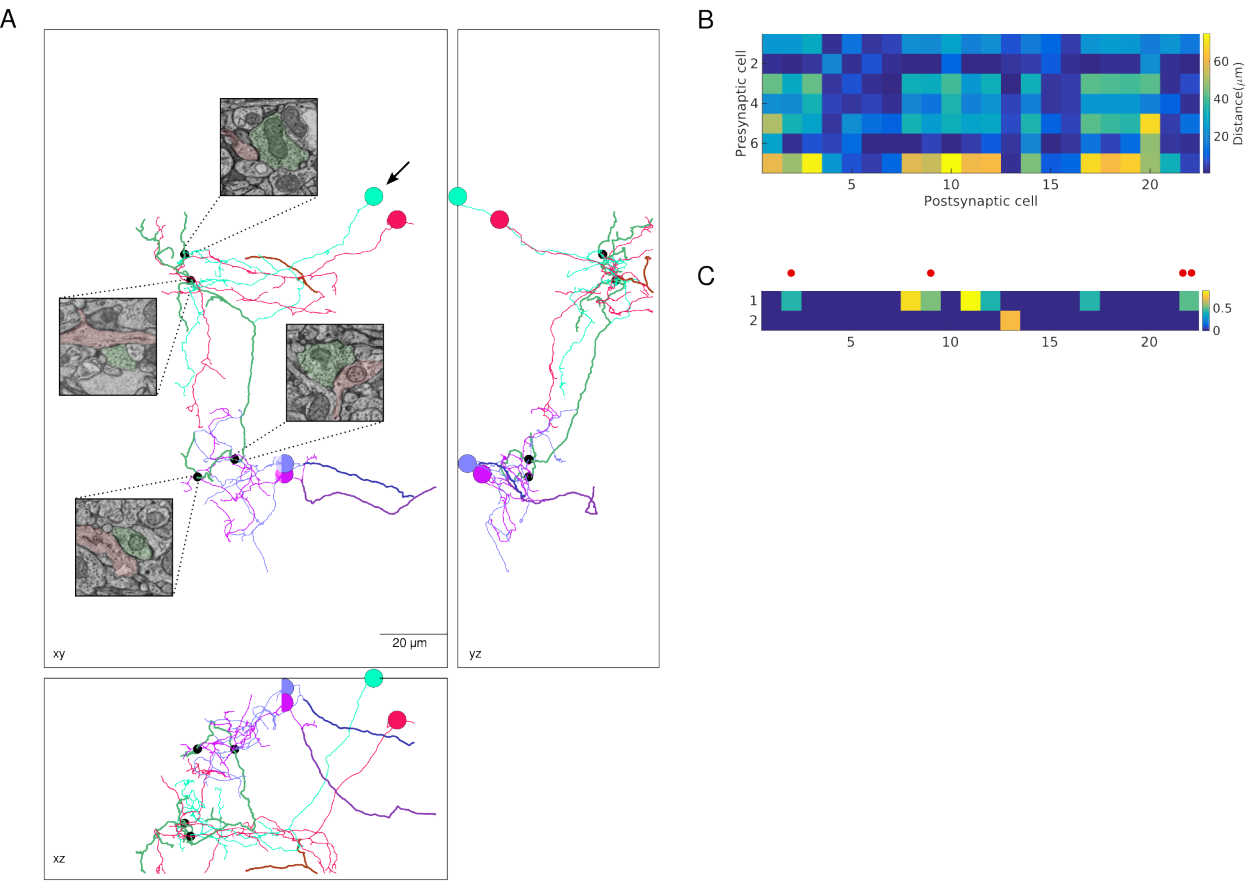


Figure 5: Synaptic connections between VPNI cells from different groups. (A) Three views of direct synaptic connections between VPNI cells from different groups. Presynaptic cell from group1 (arrow) makes synapses onto other group1 cells (pink) and onto group3 cells. (B) Minimum distance between axons of presynaptic trees and dendrites of postsynaptic trees. (C) Presynaptic trees that contain nodes that are within 1  $\mu\text{m}$  of a postsynaptic tree. Red dots are synapses that are shown in A.